Photophysical Study of Self-Assembled Donor-Acceptor Two-Layer Film on TiO_2

Kati Stranius,* Lijo George, Alexander Efimov, Tero-Petri Ruoko, Juuso Pohjola, and Nikolai V. Tkachenko*

Department of Chemistry and Bioengineering, Tampere University of Technology

E-mail: kati.stranius@tut.fi; nikolai.tkachenko@tut.fi

Phone: +358 40 198 1127. Fax: +358 3 364 1392

Abstract

The self-assembled monolayer (SAM) technique was employed to fabricate a two-layer donor-acceptor film on surface of TiO_2. The approach is based on using donor and acceptor compounds with anchoring groups of different length. The acceptor, a fullerene derivative, has a carboxyl anchor attached to the fullerene moiety *via* a short linker which places the fullerene close to the surface. The donor, a porphyrin derivative, is equipped with a long linker which can penetrate between the fullerenes and keep porphyrin on top of the fullerene layer. The two-layer fullerene–porphyrin structures were deposited on a mesoporous film of TiO_2 nanoparticles by immersing the TiO_2 film sequentially into fullerene and porphyrin solutions. Transient absorption spectroscopy studies of the samples revealed that after selective photoexcitation of porphyrin a fast (<5 ps) intermolecular electron transfer (ET) takes place from porphyrin to fullerene layer, which confirms formation of the inter-layer donor-acceptor interface. Furthermore, in the second step of ET the fullerene anions donate electrons to the TiO_2 nanoparticles. The latter reaction is relatively slow with average time constant of 230 ps.

*To whom correspondence should be addressed

It involves roughly half of primary generated charges and the second half relaxes by the inter-layer charge recombination. The resulting state with porphyrin cation and electron in the TiO_2 has extremely long lifetime and recombines with average time constant of 23 ms.

Introduction

The study of photoinduced electron transfer (ET) across a organic-semiconductor interface is driven by many promising applications such as dye sensitized[1] and hybrid solar cells,[2,3] nanophotonic devices and molecular sensors.[4] In these applications, a molecular layer is assembled on a semiconductor surface where its primary function is to capture a photon. The energy of the excited state is used then to transfer an electron across the interface in a direction determined by the energy states of the semiconductor and the molecule. Since the main role of the organic layer is photo-sensitization, relatively simple dye molecules equipped with anchor groups to attach them on the surface are typically used.

However, functionality of molecular systems is not limited to photo-sensitization, and numerous donor-acceptor (DA) molecules were designed, which can efficiently absorb the light and undergo intramolecular charge-separation.[5] Potentially such molecules can be attached to the semiconductor surface either by donor or acceptor side, so that photo-excitation will push either electron or hole towards the semiconductor. This may lead to a more efficient cross interface charge transfer or even to a control over the direction of the ET across the interface. Although utilization of DA molecules in place of simple dye photosensitizers looks promising, a number of problems stay in the way of practical implementation and a very few studies have attempted to implement this approach.[6–8] The efficient charge-separation is often impeded by the poor control over orientation and ordering of covalently linked donor-acceptor dyads in self-assembled films. Moreover, cluster formation and defects in donor-acceptor architectures fabricated by different layer-by-layer assembly methods[9] preclude efficient light energy conversion. On the other hand, co-self-assembly may lead to uneven distribution of the donors and acceptors in mixed self-assembled monolayer

films.[10,11]

Here, we propose to use donor and acceptor compounds with anchoring groups of different length as a potential approach to construct ordered DA architectures. At the first stage of deposition, acceptor molecules with a short linker form a monolayer close to the semiconductor surface. Then, donor molecules with long linker, which can penetrate between the units in the first monolayer, form second layer on top of the acceptors. This approach enables preparation of a large number of differently ordered two-layer structures only by using different combinations of donor and acceptor molecules.

Porphyrins and fullerenes are widely studied and proved to be an excellent combination for donor-acceptor pair.[5,10–14] Porphyrins are highly conjugated macrocycles which absorb light over a wide wavelength range in the visible and UV regions and have high electron donating abilities. Its activity in DA systems can be altered by changing the central atom and modifying the peripheral substituents of macrocycles.[15] Fullerene C_{60} has a high electron affinity accepting up to 6 electrons,[16] and ET reactions involving fullerenes are characterized by relatively small reorganization energy.[17] Low absorption of fullerene in the visible region makes the selective excitation of porphyrins possible and the unique anion absorption band of the fullerene in the near-IR makes detection of the ET dynamics reliable and reasonably accurate.[18] In addition, a combination of porphyrin as a donor and sensitizer with fullerene as an acceptor is known to exhibit a long-lived charge-separated (CS) state with a high quantum yield *via* photoinduced ET.[5,10,11,14] For these reasons a fullerene derivative was used to form the acceptor layer on the surface of TiO_2, and two porphyrin derivatives, free-base (**H_2P**) and zinc complex (**ZnP**), were used to deposit the top donor layer.

Experimental

Sample preparation

TiO_2 nanoparticle thin films with layer thickness of 2 μm were formed on glass substrates by a

standard doctor blade technique.[19] The substrate was framed with Scotch tape creating a 1 $\times$ 3 cm channel. Roughly 30 μl of Solaronix:Ti-Nanoxide-T paste was dropped in the channel and spread evenly with a glass rod. Resulting film was dried in air for one hour while the tape was removed after 5 min drying. After that, the samples were heated 10 minutes at 120, 250, 330, 450 and 520 °C, respectively and cooled in air.

Immobilization of the compounds on TiO_2 films was done by immersing the films in the solutions of corresponding compounds. Prior to the immobilization, TiO_2 films were heated at 150°C for 30 minutes to remove moisture. The solvent, compound concentration and immersion time were adjusted individually for each compound.

The best solvent for both **H_2P** and **ZnP** was MeOH. The concentrations of **H_2P** and **ZnP** were 0.09 mM and 0.05 mM, respectively, and the deposition time was 18 hours. After immersion the substrates were washed by immersing in neat solvent twice for one hour to remove unbonded compounds. **CF** has poor solubility in pure alcohols, thus solvent mixture of chloroform and ethanol, $CHCl_3$:EtOH = 9:1 by volume was used for the deposition. The solution concentration was 0.16 mM, immersion time 10 minutes and washing time twice for 30 minutes. The two-layer samples were prepared with two-step deposition. First, fullerene SAM was formed on TiO_2 and the plate was washed and dried in air. Then the plate was dipped into **ZnP** or **H_2P** solution to attach the donor layer and washed as above.

Steady-state spectroscopy

The UV-Vis spectra was measured with Shimadzu UV-3600 UV-VIS-NIR spectrophotometer. The fluorescence spectra were recorded with an ISA-Jobin Yvon-SPEX-Horiba Fluorolog-2-111 fluorometer and corrected using the instrument response function supplied by the manufacturer.

Transient absorption spectroscopy

A pump-probe setup was used to carry out time-resolved absorption spectroscopy studies in femtosecond time scale. In brief, the fundamental light pulses at 800 nm wavelength were generated

by a Libra F laser system (Coherent Inc.) at repetition rate of 1 kHz. The pulse energy was 1 mJ and the pulse duration was approximately 100 fs. Roughly 90% of the fundamental beam energy was delivered to the optical parametric amplifier (OPA) Topas C (Light Conversion Ltd.) to produce the pump pulses at the desired wavelength. The rest of the light was delivered to the measurement system (ExiPro, CDP Inc.) to generate white continuum for sample probing. The measurement system was equipped with two pairs of array detectors, a Si CCD arrays for measurements in the visible part of the spectrum and an InGa diode arrays for measurements in the near infrared (NIR) part of the spectrum. The white light beam, after sapphire continuum generator, was split into two beams: reference and signal. The measurements were acquired by comparing responses with and without excitation using a chopper synchronized with the fundamental laser pulses. Typical averaging time was 10 s, *i.e.* averaging 10 000 excitation shots. The spectra were recorded in two wavelength ranges 550–780 nm and 880–1100 nm. The gap between the ranges is due to high instability of the white continuum at wavelengths approching the laser fundamental. All measurements were carried out under nitrogen atmosphere.

The flash-photolysis method was used to study the time-resolved absorption in the millisecond timescale. The measurements were performed with excitation pulses from a Nd:YAG laser at 532 nm (5 ns, 5-15 mJ per pulse). The used excitation power density was ~ 0.5 mJ cm^{-2}. The monitoring light was obtained from a tungsten halogen light source (AvaLight-HAL, Avantes). The signal was detected by the silicon photoreceiver (2051-FS, New Focus) and recorded by the digitizing oscilloscope TDS3032B (Tektronix, 300 MHz). The Luzchem laser flash system (mLFP-111) was used to control the experiments. The transient decays were collected in the wavelength range from 450 nm to 900 nm in a nitrogen atmosphere.

Multiexponential or combination of exponential and distributed decay models was used for global fit of the data obtained from transient absorption measurements.[20,21] In some cases a short, < 100 fs, component was needed for the fitting. This component is at the limit of the instruments time resolution and most probably originates from imperfection of the dispersion compensation and estimation of the instrument response function. Thus those components have no physical

meaning and were left outside of the discussion.

Results

Compounds

Chemical structures of the compounds, carboxy-substituted porphyrins, **H_2P** and **ZnP**, and fullerene derivative **CF** are presented in Figure 1. The details of synthesis, purification and characterization are provided in Supporting Information. The absorption spectra of the porphyrins, **H_2P** and **ZnP**, in MeOH and fullerene **CF** in $CHCl_3$:EtOH (9:1) are presented in Figure 2.

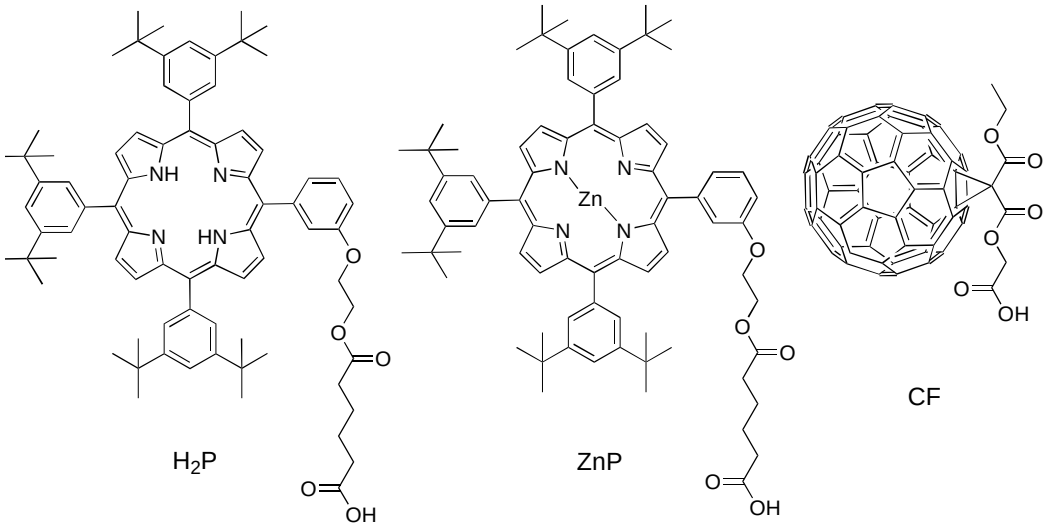

Figure 1: Chemical structures of carboxy-substituted free-base porphyrin, **H_2P**, zinc porphyrin, **ZnP** and fullerene, **CF**.

Mono- and two-layer films

SAMs were deposited on TiO_2 nanoparticle films of roughly 2 μm thickness by immersing the TiO_2 films into solutions of organic molecules. The layer formation was controlled by measuring the film absorption. A critical parameter for the deposition of SAMs of **CF** was immersion time. Absorption of the samples increases with increasing immersion time until 15 minutes, and does not grow much after that, as illustrated in Figure 3a. A slightly wavy shape of the spectra in the

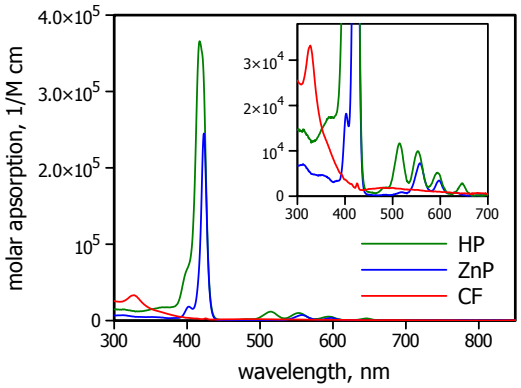

Figure 2: Absorption spectra of **CF** in $CHCl_3$:EtOH (9:1) and **H_2P** and **ZnP** in MeOH. Inset shows the magnified spectra to visualize the Q-band part of the spectrum better.

figure is due to the light interference in the TiO_2 layer, and it was observed for all samples. After deposition, the samples were only quickly washed by dipping them in pure solvent ($CHCl_3$:EtOH mixture). A more thorough washing of the samples causes a loss of the sample absorption. As shown in Figure 3b, after one hour of keeping the sample in neat solvent the absorption decreases by half. However, further washing does not change the sample absorption any more.

Based on these results, **CF** SAMs were prepared by immersing TiO_2 films in the solution for 10 minutes and then washing in pure solvent twice for 30 minutes each time. One can also notice that absorption spectra of **CF** samples are rather featureless with absorbance increasing gradually toward shorter wavelengths. This is typical for densely packed fullerene films.[22]

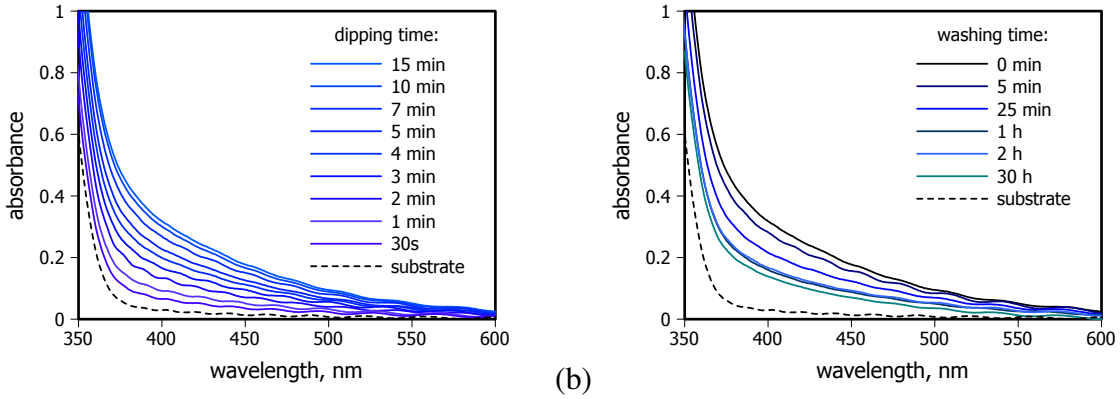

Figure 3: Absorption spectra of **CF** monolayer on TiO_2 (a) after different immersion times and quick rinsing of the samples and (b) after different washing times. The immersion time is indicated in the plot.

Similar studies were carried out for **H_2P** and **ZnP** (see Supporting Information, Figures S1–S2). Though these compounds form more stable layers, the rate of SAM formation for both porphyrin derivatives was much lower. Thus, much longer, 18 hours, immersion time was used to deposit the layers and after deposition the samples were washed in pure MeOH twice for one hour each time.

Absorption spectra of single and two-layer structures of **H_2P** and **ZnP**, and **CF | H_2P** and **CF | ZnP**, respectively, are presented in Figure 4. Absorption of the samples at Soret band of porphyrins are much higher than the maximum measurable value for the instrument used. However, the Q band region is seen well with maximum absorptance in the range $0.2-0.5$, which is suitable for conducting transient absorption measurements by the pump-probe method. The absorption of porphyrin in **CF | ZnP** and **CF | H_2P** structures is roughly 30% lower than that of porphyrin layer alone. This is an expected result as the packing of porphyrins on top of the fullerene layer cannot be as dense as on clean TiO_2 surface, since much lower density of potential binding sites is available for the anchor groups of porphyrin derivatives in this case.

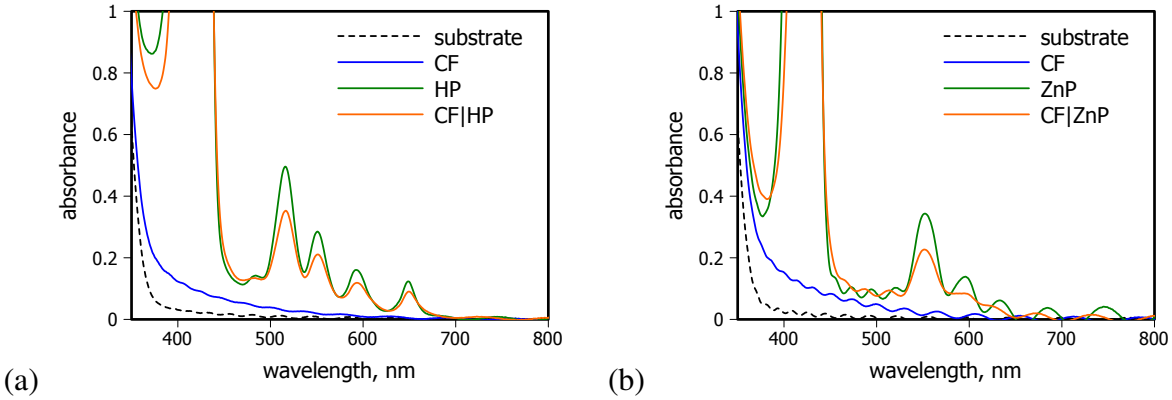

Figure 4: Absorption spectra of (a) **CF** and **H_2P** monolayers and **CF | H_2P** two-layer structures and (b) **CF** and **ZnP** monolayers and **CF | ZnP** two-layer structures on TiO_2.

The selective excitation of porphyrin chromophore in two-layer structures is possible in Q-band area and thus the most intense Q-bands, at 515 nm for **H_2P** and 555 nm for **ZnP**, were used for photoexcitation. The fluorescence intensity of both **H_2P** and **ZnP** is decreased by roughly 70% in two-layer structures as compared with porphyrin SAMs deposited directly on TiO_2 surface (see

Supporting Information, Figures S3–S4). The emission of porphyrin SAMs on TiO_2 is probably already quenched due to their aggregation in the SAM and possible ET to TiO_2, but the enhanced quenching on top of **CF** layer indicates relatively strong electronic interactions between the two organic layers.

Transient absorption

The transient absorption responses of all the samples with porphyrin layer were measured by exciting porphyrins selectively at the shorter wavelength Q-bands, 515 and 555 nm for $\mathbf{H_2P}$ and **ZnP**, respectively. To study the photo-response of the **CF** layer alone, the excitation wavelength of 400 nm was used. At this wavelength **CF** absorbance is only 0.15. The absorbance is higher at shorter wavelengths, but the absorbance of TiO_2 film also increases sharply toward the shorter wavelengths, and 400 nm was selected as a reasonable compromise between the excitation selectivity and efficiency. Figure 5 shows the time-resolved differential absorption spectra with compensated group velocity dispersion for TiO_2 | **CF** sample. The broad non-structured spectrum is typical for the fullerene excited singlet state.[23] The singlet state relaxes non-exponentially to the ground state with average time constant close to 100 ps, and at 5 ns delay time no transient absorption can be detected. The shape of the transient spectrum does not change in time, which means that the singlet excited state of fullerene relaxes directly to the ground state through the intermolecular interactions in aggregated film. Similar decays were observed also for a drop cast **CF** film on glass substrate (see Supporting Information, Figure S5).

The results of transient absorption measurements of **ZnP** on TiO_2 are presented in Figure 6. A four-exponential global fit gave reasonably good approximation of the data, and the spectra of components associated with the four time constants are presented in Figure 6a. The time-resolved absorption spectra at a few delay times are presented in Figure 6. The spectrum at 0.1 ps delay time refers to the differential spectrum right after the excitation. Its noticeable features are dips at 605 and 660 nm, which are characteristic for the first singlet excited state of **ZnP**.[24] These dips correspond to the bleaching of the ground state absorption, namely the Q-band at 605 nm,

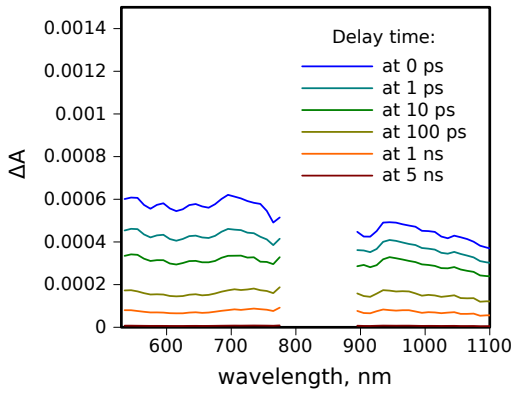

Figure 5: Time-resolved transient absoption spectra of **CF** monolayer on TiO_2.

and stimulated emission at the lower energy emission band of the porphyrin at 660 nm. The two shorter-lived components (4 and 30 ps) have rather similar spectra and both indicate recovery of the spectral dip at 660 nm, which means that they both can be attributed to relaxation of the singlet excited state. The relaxation is not mono-exponential since there are variations of local environments and molecular arrangements co-existing in the SAM.[24,25]

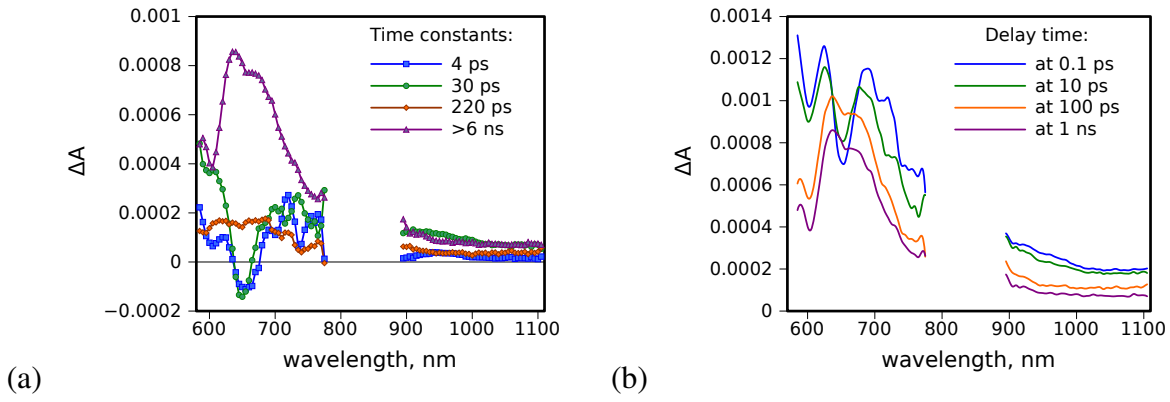

(a) (b)

Figure 6: Transient absorption decay component spectra (a) and time-resolved transient absorption spectra (b) of **ZnP** monolayer on TiO_2.

The state left after the singlet state relaxation has a spectrum typical for **ZnP** cations with a clear absorption band in the 650-700 nm region,[12,26] as seen for the time-resolved spectrum at 100 ps in Figure 6b. This is an expected result as photoexcited zinc porphyrins are known to eject electrons to the TiO_2 conduction band.[19,24,27] In our case, the process of electron injection is relatively slow (4-30 ps) compared to results published for other zinc porphyrin layers on TiO_2,

which is explained by a long linker connecting **ZnP** to TiO_2. At the same time, longer linker increases the lifetime of the porphyrin cation. There is virtually no decay of the cation in the time window of pump-probe measurements, 6 ns, except of relatively minor decay component with the time constant of 220 ps (Figure 6a).

The transient absorption measurements for $\mathbf{H_2P}$ on TiO_2 show similar spectral changes, though the singlet state relaxation is slower and the efficiency of ET is lower (Figure 7). The initial state formed after excitation (time-resolved spectrum at 1 ps) is the porphyrin singlet excited state, as expected. The differential spectrum of this state shows bleaching of the Q bands and a dip at 720 nm, a wavelength corresponding to the lower energy emission band. The singlet state decays with 400 ps time constant yielding a low intensity spectrum with a broad absorption band in the 600-700 nm region. The latter can be attributed to porphyrin cation, H_2P^+.[26] There is also a fast, ~ 0.1 ps, decay component which is most probably due to a fast thermal relaxation for porphyrin to the lowest vibrational state of the first singlet excited state.

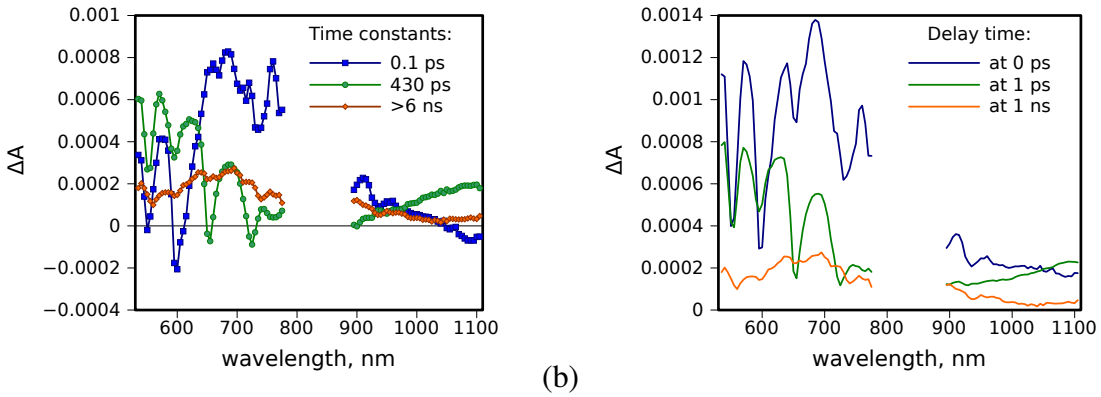

(a) (b)

Figure 7: Transient absorption decay component spectra (a) and time-resolved transient absorption spectra (b) of $\mathbf{H_2P}$ monolayer on TiO_2.

The transient absorption response of TiO_2 | **CF** | **ZnP** sample was rather complex and at least five-exponential approximation was needed for reasonable data fitting. In addition, it was noticed that the spectra of some exponential components are quite similar, which indicates that the transitions between states do not follow exponential law. At the qualitative level, the time-resolved spectra (Figure 8b) have relatively straightforward interpretation. The state at long delay, 2 ns, can

be attributed to **ZnP** cation. Its characteristic features are an absorption band at $\sim$ 640 nm, a dip at 605 nm which corresponds to the bleached lowest energy Q-band and almost no absorption in the near IR part of the spectrum. This spectrum is also almost identical to that of TiO_2 | **ZnP** sample at long delay time (at 1 ns, Figure 6b), and can be assigned to porphyrin cation, ZnP^+. However the formation process of ZnP^+ is different in two films.

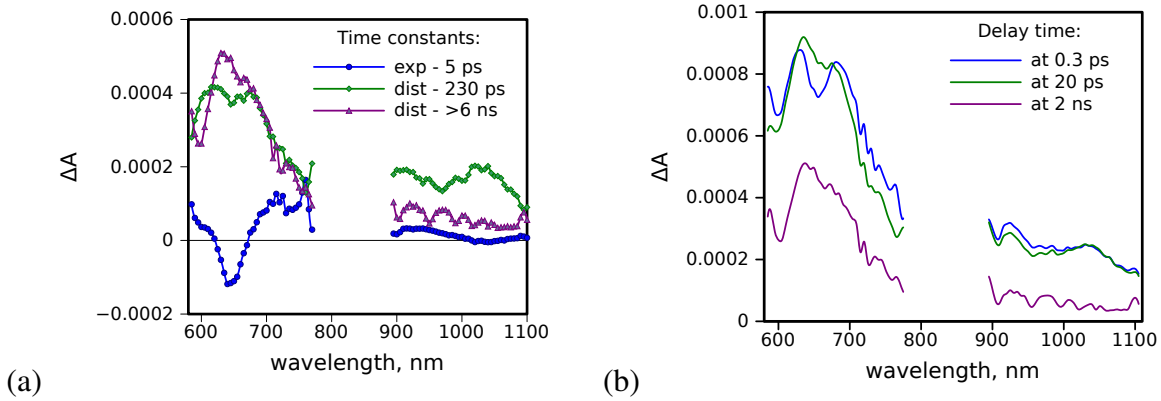

(a) (b)

Figure 8: Transient absorption decay component spectra (a) and time-resolved transient absorption spectra (b) of **CF** | **ZnP** film on TiO_2.

The first time-resolved spectrum of the TiO_2 | **CF** | **ZnP** sample has already a band in 600–700 nm region and relatively shallow dips at 605 and 660 nm, which are the singlet exited state indicators. There is also significant absorption in the near IR part of the spectrum with a band at 1050 nm. The dip at 660 nm disappears with roughly 5 ps time constant and the band at 1050 nm becomes more pronounced. The latter band is typical for fullerene anion, and the spectrum at 20 ps delay can be attributed to the intermolecular charge separated (CS) state, ZnP^+-C_{60}^-.

Assignment of the spectrum at 0.3 ps cannot be done if only one of possible precursors of the CS state is considered. Firstly, comparing the time-resolved spectra of TiO_2 | **CF** | **ZnP** and TiO_2 | **ZnP** (Figure 6b) at short delay times, at 0.3 and 0.1 ps, respectively, one can notice that the spectral features of the porphyrin singlet excited state are less pronounced in the two-layer sample. The difference between the two short delay spectra is that the response of the two-layer sample is closer spectrally to the CS state. Most probably many types of porphyrin–fullerene arrangements coexist in this film and the intermolecular CS proceed with different time constants

in the range from 100 fs to a few picoseconds. As the result, the first time-resolved spectrum is already a mixture of the primary excited porphyrins and CS states. Alternatively, the first spectrum can be a mixture of the porphyrin singlet excited state and intermolecular porphyrin–fullerene exciplex, which is known to form in few hundreds of femtoseconds in face-to-face porphyrin–fullerene dyads.[28]

With this knowledge of possible photo-reactions in TiO_2 | **CF** | **ZnP** sample, the transient absorption data were fitted using a combination of exponential and distributed decay models, used previously to analyze ET in porphyrin–fullerene and phthalocyanine–fullerene dyad films.[20,21] A reasonable approximation was achieved with two exponential and two distributed decay components which gave a sigma-value better than that from the five exponential fitting. The decay component spectra are presented in Figure 8a, except for the fast, 0.1 ps, component.

The second exponential component with 5 ps time constant resembles very much those corresponding to 4 and 30 ps components in the case of TiO_2 | **ZnP** sample (Figure 6a) in the visible part of the spectrum, and shows also the 1050 nm band reshaping in the near IR part. This can be attributed to the relaxation of the remaining part of the singlet excited state by yielding the intermolecular CS state, ZnP^+-C_{60}^-. The CS process is most probably non-exponential, but use of a more complex model did not improve the quality of the fit.

The most interesting result of the fit is the spectra of two distributed decay component. The components are very much similar and have roughly the same intensities in the visible part of the spectrum. However, in the near IR part the spectra are very different. The 230 ps component has a distinct band at 1050 nm and can be attributed to the decay of intermolecular CS state. The second component has a lifetime much longer than the maximum delay time of the instrument, 6 ns, and has practically no absorption in the near IR part of the spectrum. This component represents porphyrin cation spectrum alone showing no sign of fullerene anion. Apparently, this state is formed as the result of electron injection from fullerene anion to TiO_2. Thus the time constant of 230 ps results from two competing processes, the electron injection to TiO_2 and intermolecular charge recombination. The two distributed decay time constant are well separated from each other,

which made the qualitative prediction of the photoreactions taking place in the sample possible based on the time-resolved spectra.

The long-lived components from the pump-probe measurements were longer than the longest delay available from the instrument, 6 ns, for both, TiO_2 | **ZnP** and TiO_2 | **CF** | **ZnP**. Thus, the nanosecond flash-photolysis instrument was used to measure transient absorption of the samples in the time scale up to hundreds of milliseconds The excitation wavelength was 532 nm. At this wavelength, **ZnP** was excited predominantly, though the absorption of **ZnP** was really low. A reasonable fit was achieved with one exponential and one distributed decay components. The exponential component had a lifetime shorter than the time resolution of the instrument and was needed to account for the instrument response. The spectrum of the distributed decay component obtained from the flash-photolysis measurement corresponds well to that of the longest-lived component obtained from the pump-probe measurements and attributed to ZnP^+ (Figure 9). The obtained average time constants were 6.2 and 23 ms for TiO_2 | **ZnP** and TiO_2 | **CF** | **ZnP** samples, respectively.

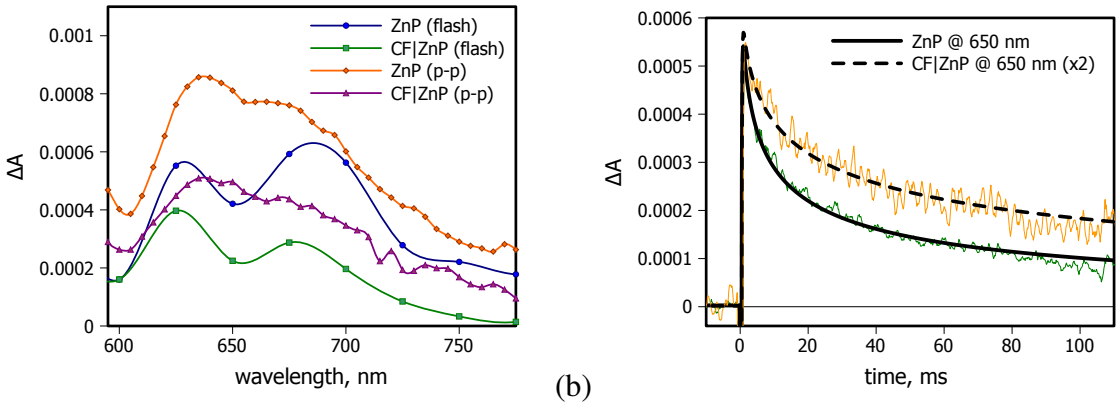

(a) (b)

Figure 9: (a) Spectra of the longest-living components obtained from the pump-probe and flash-photolysis measurements and (b) transient absorption decay curves at 650 nm from the flash-photolysis measurements for **ZnP** monolayer and **CF** | **ZnP** two-layer films on TiO_2.

The results of measurements of similar two-layer structure with free-base porphyrin, TiO_2 | **CF** | $\mathbf{H_2P}$, are presented in Supporting Information (Figure S7). The longest-lived component has shape similar to the longest-lived component observed for porphyrin only sample and can be attributed to porphyrin cation, H_2P^+. However the component with with 1.3 ns lifetime has a broad and almost

featureless spectrum, resembling the time-resolved spectra observed for the fullerene only sample, and is therefore attributed to fullerene singlet excited state. The 43 ps and 210 ps components are again similar to the 430 ps component observed for porphyrin only sample and are attributed to a bi-exponential relaxation of the porphyrin singlet excited state. Unlike the samples with zinc porphyrin, there are no evidences of free-base porphyrin-fullerene ET, since there are no spectral component resembling the CS state or intermolecular exciplex. In addition, the observed component spectra of the two-layer sample have their analogues in component spectra of monolayer porphyrin and fullerene samples. The only indirect evidence of porphyrin–fullerene interaction is the shorter lifetime of the porphyrin singlet excited state, which is most probably due to the porphyrin–fullerene energy transfer. The energy transfer explains the enhanced emission quenching and the appearance of a detectable amount of the excited state of fullerene (1.3 ns component) since the excitation at 515 nm is very inefficient in exciting fullerenes directly.

Discussion

All the films were prepared following exactly the same protocol and the specific areas are expected to be the same for all the samples. Therefore relative absorption intensities of the samples can be compared to get an estimation of relative densities of the molecular layers on TiO_2 surfaces. Average absorbance of the **CF** SAMs on TiO_2 is 0.15 at 400 nm. Absorbance of the $\mathbf{H_2P}$ SAM is 0.5 and absorbance of the **CF** | $\mathbf{H_2P}$ samples is 0.3 at 515 nm. Considering that the molar absorption of these molecules at these wavelengths are $\varepsilon_{CF} \approx 3500$ $M^{-1}cm^{-1}$ and $\varepsilon_{HP} \approx 11300$ $M^{-1}cm^{-1}$ for **CF** and $\mathbf{H_2P}$, respectively, the surface densities of molecules in single layer SAMs are roughly the same. However, in the two-layer samples the ratio of molecules **CF**:$\mathbf{H_2P}$ is roughly 3:2. Molar absorption of **ZnP** at 555 nm is $\varepsilon_{ZnP} \approx 6800$ $M^{-1}cm^{-1}$, and the monolayer and two-layer sample absorbances are 0.35 and 0.2, respectively, at 559 nm. Thus the density of **ZnP** molecules in monolayer SAM is approximately the same as in monolayer SAMs of **CF** and $\mathbf{H_2P}$, and in the case of two-layer SAM the ratio is **CF**:**ZnP** $\approx$ 3:2, which is the same as for **CF** | $\mathbf{H_2P}$ samples. The

lower density of porphyrin layer deposited on top of the fullerenes as compared to that on clean TiO_2 surface is the expected outcome, since after **CF** deposition the density of available binding points on the surface is lower and packing of porphyrins atop of fullerenes cannot be as high as on an open surface.

According to the intensities of transient absorption spectra of the singlet excited state and porphyrin cation of TiO_2 | **ZnP** sample, the efficiency of the electron injection from porphyrin to the conduction band of TiO_2 is essentially lower than 100%. Typically the cation absorption at 700 nm is two times higher than that of the singlet state.[23] The observed intensity of the cation (the spectrum at 100 ps delay, Figure 6b), is somewhat lower that the intensity of the singlet state absorption (the spectrum at 0.1 ps, Figure 6b). This leads to an estimation that the efficiency of the ET is approximately 30%. The rest of photo-excited molecules decay non-radiatively to the ground state. The average time constant of the singlet state relaxation is about 20 ps.

In the case of the TiO_2 | **CF** | **ZnP** structure, the primary relaxation of the porphyrin singlet state is at the limit of the instrument time resolution at least for half of the excited porphyrins, and the first time resolved spectrum (the spectrum at 0.3 ps, Figure 8b) has a less intense dip at 650 nm compared to that of the TiO_2 | **ZnP** sample (Figure 6b). The dip at 650 nm is a characteristic feature of the porphyrin singlet excited state and this observation indicates that over half of the primary excited singlet state decays within 300 fs time interval. This decay does not lead to decrease of the absorption in the 600-700 nm region, but rather it gives rise to the absorption in this region. The decay of the remaining singlet excited states, which relax with 5 ps time constant, contributes also to somewhat high absorption in this range. This shows that close to 100% of the singlet state is converted to a new state, which can be either intermolecular porphyrin-fullerene exciplex, $(ZnP\text{-}C_{60})^*$, or the CS state, $ZnP^+\text{-}C_{60}^-$. This is the first important difference to the monolayer TiO_2 | **ZnP**: the two-layer sample has no any detectable relaxation to the ground state during the singlet state relaxation. Secondly, the average lifetime of the singlet state is not longer than 5 ps for the **CF** | **ZnP** sample, whereas for the monolayer sample the average lifetime is 20 ps. These two observations are in agreement with each other, and prove the close contact between porphyrin and

fullerene in two-layer samples – most of the excited porphyrins interact efficiently with fullerenes by yielding the CS state. This ET is manifested by the fullerene anion band in the near IR part of the spectrum (Figure 8). According to the transient absorption measurements, the quantum yield of the CS state is close to 100% since there is no detectable decay of the transient absorption prior to the CS state formation.

The average lifetime of the intermolecular CS state is 230 ps. Its decay leads to complete disappearance of the fullerene anion band in the near IR and only partial decay of porphyrin cation band in the visible part of the spectrum (see Supporting Information, Figure S6, for the decay comparison at two wavelengths). This is possible only if the fullerene anion donates an electron to the conduction band of TiO_2. The efficiency of this process is roughly 60% as can be estimated from comparison of the decay component spectra corresponding to 230 ps and 20 ns components (Figure 8a) or time-resolved spectra at 20 ps and 2 ns (Figure 8b). Apparently the ET from fullerene anion to TiO_2 is much slower than that from porphyrin singlet excited state, though the expected distance between **CF** and TiO_2 is shorter than that between **ZnP** and TiO_2 in the monolayer sample. If one considers only the lowest energy level of the TiO_2 conduction band as the electron accepting level, the driving force for the ET is lower for TiO_2 | C_{60}^- pair than that for TiO_2 | ZnP^{1S} pair. For ET in the normal Marcus region this results in slower ET. The second reason for slower ET for TiO_2 | C_{60}^- pair is the fact that there are many energy levels in the conduction band. In this case a lower energy of the electron donor, C_{60}^-, means that there are fewer potential electron accepting states of the acceptor, TiO_2, which also leads to slower ET in otherwise similar conditions. Considering that the excited state is less efficient electron donor than the anion, inefficient electron injection from the photoexcited fullerene to TiO_2 (TiO_2 | **CF** sample) is very reasonable outcome as the excited state lifetime is only 100 ps.

In both samples, TiO_2 | **ZnP** and TiO_2 | **CF** | **ZnP**, the final state is ZnP^+. However, the measured lifetime for ZnP^+ is almost four times longer for TiO_2 | **CF** | **ZnP** sample ($\approx$ 23 ms) than for TiO_2 | **ZnP** sample ($\approx$ 6.2 ms). In both cases the distance between **ZnP** and TiO_2 is relatively large which leads to rather slow charge recombination. Most probably the recombination

in TiO_2 | **ZnP** sample is faster because the separation is shorter in this sample as the linker has more freedom for bending which reduces the distance.

Although the difference between free-base and zinc porphyrins is very minor, and at least exciplex was previously observed for free-base porphyrin-fullerene dyads, no evidence for porphyrin-fullerene interaction was observed for TiO_2 | **CF** | $\mathbf{H_2P}$ samples. Apparently formation of two-layer donor-acceptor film was not as effective for the free-base porphyrin as for the zinc counterpart, though the reason for this is not clear.

Zinc porphyrin derivatives have been widely studied in dye sensitized solar cell applications and in particular dynamics of the electron injection to TiO_2 and charge recombination were measured by time resolved spectroscopy techniques.[3,19,24,27,29] A comparison can be made with results reported here, though a notice has to be made that most previously reported measurements were conducted with samples placed in a solution. It seems to be well accepted that the fastest electron injection from porphyrin to TiO_2 takes place for porphyrins at relatively short distance from the surface, e.g. provided by one phenyl spacer, and slightly tilted orientation of macrocycle.[19,24,27] Then the electron injection is taking place in less than 1 ps. Reported here TiO_2 | **ZnP** system cannot provide the optimum geometry and the electron injection is much slower, 4–20 ps. However, the goal of this study was to build up two-layer donor-acceptor structure on TiO_2 surface with fast and efficient primary charge separation in the organic film. This goal was achieved and the most of excited porphyrins donate electron to fullerene in less than 0.3 ps. Though the second step, the electron injection to TiO_2 is slow ($\approx$ 230 ps) and less efficient ($\approx$ 60%). The most probable reason for slow injection is relatively low driving force, which is the energy difference between lower edge of TiO_2 conduction band and LUMO level of fullerene as indicated in Figure 10. The reported energies of the TiO_2 conduction band varies in the range $-4.4 \ldots -4.2$ eV,[2,30] and LUMO of fullerene was estimated to be around -4.1 eV.[31,32] The faster electron injection would require acceptor with higher LUMO, and actually was achieved for the TiO_2 sensitized by the covalently linked porphyrin-pthalocyanide dyad.[33] In the latter case the injection of the electron form porphyrin anion is taking place in roughly 30 ps, though comparison between these two donor-

acceptor layers on TiO_2 is not straightforward as the layers have very different structure and were prepared by different methods.

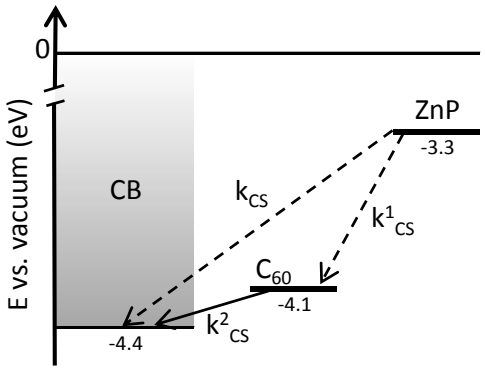

Figure 10: Schematic representation of potential energy diagram of TiO_2 | **ZnP** and TiO_2 | **CF** | **ZnP**. k_{CS} refers to the electron injection directly from **ZnP** to TiO_2 in TiO_2 | **ZnP** sample and k^1_{CS} and k^2_{CS} to the electron transfer inside the organic layer and from **CF** to TiO_2, respectively.

Conclusions

A new method for deposition of donor-acceptor two-layer molecular films using self-assembling approach is proposed and used to construct DA film on TiO_2 surface. The method is based on using two compounds with different length of linkers responsible for the layer self-assembling. First, fullerene equipped with a short linker forms the primary SAM on TiO_2. After that, porphyrin with a long linker can form the secondary layer on top of the fullerenes.

Porphyrins showed stable layer formation on top of the primary fullerene layer indicating the successful anchoring to TiO_2 *via* a carboxylic acid linker penetrating between the fullerenes in the primary SAM. Also the density of porphyrin molecules in the two-layer structure was roughly 30% lower than in the monolayer deposited directly on TiO_2. The transient absorption measurements with selective excitation of porphyrin layer revealed efficient interlayer charge separation manifested by porphyrin cation and fullerene anion bands in TiO_2 | **CF** | **ZnP** sample. This confirms formation of the two-layer structure in which most of the porphyrins were located on top of the

fullerene layer. The primary charge separation between the fullerene and porphyrin layers was followed by the electron transfer from the fullerene anion to TiO_2 with average time constant of 230 ps and efficiency close to 60%.

Importantly, the lifetime of the charge separation increased gradually to ca. 20 ms as compared with porphyrin monolayer films and specially with those having short linker, which are typically used in dye sensitized solar cells. This can be attributed to a much longer separation distance between the semiconductor holding an electron and porphyrin cation.

The proposed method can be used to easily construct the ordered two-layer donor-acceptor structures with different combinations of donors and acceptors or molecules with other functions to enhance the functionality of organic layers on semiconductor surfaces.

Acknowledgement

The authors thank Academy of Finland (grants No 263486 and 270308) and The National Doctoral Programme in Nanoscience (NGS-NANO) for funding.

Supporting Information Available

Details of synthesis, purification and characterization of all molecules; absorption spectra of the samples after different washing times; fluorescence spectra and transient absorption curves.

This material is available free of charge via the Internet at `http://pubs.acs.org/`.

References

(1) Gong, J.; Liang, J.; Sumathy, K. Review on Dye-Sensitized Solar Cells (DSSCs): Fundamental Concepts and Novel Materials. *Ren. Sust. Energ. Rev.* **2012**, *16*, 5848–5860.

(2) Wright, M.; Uddin, A. Organic-Inorganic Hybrid Solar Cells: A Comparative Review. *Sol. Energy Mater. Sol. Cells* **2012**, *107*, 87–111.

(3) Imahori, H.; Umeyama, T.; Ito, S. Large π-Aromatic Molecules as Potential Sensitizers for Highly Efficient Dye-Sensitized Solar Cells. *Acc. Chem. Res.* **2009**, *42*, 1809–1818.

(4) Naaman, R. Molecular Controlled Nano-Devices. *Phys. Chem. Chem. Phys.* **2011**, *13*, 13153–13161.

(5) Bottari, G.; Trukhina, O.; Ince, M.; Torres, T. Towards Artificial Photosynthesis: Supramolecular, Donor-Acceptor, Porphyrin- and Phthalocyanine/Carbon Nanostructure Ensembles. *Coord. Chem. Rev.* **2012**, *256*, 2453–2477.

(6) Fungo, F.; Otero, L.; Borsarelli, C. D.; Durantini, E. N.; Silber, J. J.; Sereno, L. Photocurrent Generation in Thin SnO_2 Nanocrystalline Semiconductor Film Electrodes from Photoinduced Charge-Separation State in Porphyrin-C_{60} Dyad. *J. Phys. Chem. B* **2002**, *106*, 4070–4078.

(7) Yamada, H.; Imahori, H.; Nishimura, Y.; Yamazaki, I.; Ahn, T. K.; Kim, S. K.; Kim, D.; Fukuzumi, S. Photovoltaic Properties of Self-Assembled Monolayers of Porphyrins and Porphyrin- Fullerene Dyads on ITO and Gold Surfaces. *J. Am. Chem. Soc.* **2003**, *125*, 9129–9139.

(8) Chukharev, V.; Vuorinen, T.; Efimov, A.; Tkachenko, N. V.; Kimura, M.; Fukuzumi, S.; Imahori, H.; Lemmetyinen, H. Photoinduced Electron Transfer in Self-Assembled Monolayers of Porphyrin-Fullerene Dyads on ITO. *Langmuir* **2005**, *21*, 6385–6391.

(9) Ariga, K.; Yamauchi, Y.; Rydzek, G.; Ji, Q.; Yonamine, Y.; Wu, K. C.-W.; Hill, J. P. Layer-by-layer Nanoarchitectonics: Invention, Innovation, and Evolution. *Chem. Lett.* **2014**, *43*, 36–68.

(10) Imahori, H.; Mori, Y.; Matano, Y. Nanostructured Artificial Photosynthesis. *J. Photochem. Photobiol. C* **2003**, *4*, 51–83.

(11) Li, M.; Ishihara, S.; Ji, Q.; Akada, M.; Hill, J. P.; Ariga, K. Paradigm Shift from Self-

Assembly to Commanded Assembly of Functional Materials: Recent Examples in Porphyrin/Fullerene Supramolecular Systems. *Sci. Tech. Adv. Mater.* **2012**, *13*, 053001.

(12) Kuciauskas, D.; Lin, S.; Seely, G. R.; Moore, A. L.; Moore, T. A.; Gust, D.; Drovetskaya, T.; Reed, C. A.; Boyd, P. D. W. Energy and Photoinduced Electron Transfer in Porphyrin-Fullerene Dyads. *J. Phys. Chem.* **1996**, *100*, 15926–15932.

(13) Imahori, H.; Sakata, Y. Fullerenes as Novel Acceptors in Photosynthetic Electron Transfer. *Eur. J. Org. Chem.* **1999**, *1999*, 2445–2457.

(14) El-Khouly, M. E.; Ito, O.; Smith, P. M.; D'Souza, F. Intermolecular and Supramolecular Photoinduced Electron Transfer Processes of Fullerene-Porphyrin/Phthalocyanine Systems. *J. Photochem. Photobiol. C* **2004**, *5*, 79–104.

(15) Smith, K. M.; Falk, J. E. *Porphyrins and Metalloporphyrins*; Elsevier: Amsterdam, 1975.

(16) Echegoyen, L.; Echegoyen, L. E. Electrochemistry of Fullerenes and Their Derivatives. *Acc. Chem. Res.* **1998**, *31*, 593–601.

(17) Imahori, H.; Tkachenko, N. V.; Vehmanen, V.; Tamaki, K.; Lemmetyinen, H.; Sakata, Y.; Fukuzumi, S. An Extremely Small Reorganization Energy of Electron Transfer in Porphyrin-Fullerene Dyad. *J. Phys. Chem. A.* **2001**, *105*, 1750–1756.

(18) Kirner, S.; Sekita, M.; Guldi, D. M. 25th Anniversary Article: 25 Years of Fullerene Research in Electron Transfer Chemistry. *Adv. Mater.* **2014**, *26*, 1482–1493.

(19) Ye, S.; Kathiravan, A.; Hayashi, H.; Tong, Y.; Infahsaeng, Y.; Chabera, P.; Pascher, T.; Yartsev, A. P.; Isoda, S.; Imahori, H.; Sundström, V. Role of Adsorption Structures of Zn-Porphyrin on TiO_2 in Dye-Sensitized Solar Cells Studied by Sum Frequency Generation Vibrational Spectroscopy and Ultrafast Spectroscopy. *J. Phys. Chem. C* **2013**, *117*, 6066–6080.

(20) Lehtivuori, H.; Efimov, A.; Lemmetyinen, H.; Tkachenko, N. V. Distributed Decay Kinetics of Charge Separated State in Solid Films. *Chem. Phys. Lett.* **2007**, *437*, 238–242.

(21) Lehtivuori, H.; Kumpulainen, T.; Efimov, A.; Lemmetyinen, H.; Kira, A.; Imahori, H.; Tkachenko, N. V. Photoinduced Electron Transfer in Langmuir–Blodgett Monolayers of Double-Linked Phthalocyanine–Fullerene Dyads. *J. Phys. Chem. C* **2008**, *112*, 9896–9902.

(22) Guldi, D. M.; Luo, C.; Koktysh, D.; Kotov, N. A.; Ros, T. D.; Bosi, S.; Prato, M. Photoactive Nanowires in Fullerene-Ferrocene Dyad Polyelectrolyte Multilayers. *Nano Lett.* **2002**, *2*, 775–780.

(23) Kesti, T. J.; Tkachenko, N. V.; Vehmanen, V.; Yamada, H.; Imahori, H.; Fukuzumi, S.; Lemmetyinen, H. Exciplex Intermediates in Photoinduced Electron Transfer of Porphyrin-Fullerene Dyads. *J. Am. Chem. Soc.* **2002**, *124*, 8067–8077.

(24) Imahori, H.; Kang, S.; Hayashi, H.; Haruta, M.; Kurata, H.; Isoda, S.; Canton, S. E.; Infahsaeng, Y.; Kathiravan, A.; Pascher, T.; Chabera, P.; Yartsev, A. P.; Sundström, V. Photoinduced Charge Carrier Dynamics of Zn-Porphyrin-TiO_2 Electrodes: The Key Role of Charge Recombination for Solar Cell Performance. *J. Phys. Chem. A* **2011**, *115*, 3679–3690.

(25) Asbury, J. B.; Hao, E.; Wang, Y.; Ghosh, H. N.; Lian, T. Ultrafast Electron Transfer Dynamics from Molecular Adsorbates to Semiconductor Nanocrystalline Thin Films. *J. Phys. Chem. B.* **2001**, *105*, 4545–4557.

(26) Gasyna, Z.; Browett, W. R.; Stillman, M. J. p-Cation-Radical Formation Following Visible Light Photolysis of Porphyrins in Frozen Solution Using Alkyl Chlorides or Quinones as Electron Acceptors. *Inorg. Chem.* **1985**, *24*, 2440–2447.

(27) Hart, A. S.; KC, C. B.; Gobeze, H. B.; Sequeira, L. R.; D'Souza, F. Porphyrin-Sensitized Solar Cells: Effect of Carboxyl Anchor Group Orientation on the Cell Performance. *ACS Appl. Mater. Interfaces* **2013**, *5*, 5314–5323.

(28) Chukharev, V.; Tkachenko, N. V.; Efimov, A.; Guldi, D. M.; Hirsch, A.; Scheloske, M.; Lemmetyinen, H. Tuning the Ground-State and Excited-State Interchromophore Interactions in Porphyrin-Fullerene π-Stacks. *J. Phys. Chem. B* **2004**, *108*, 16377–16385.

(29) Hakola, H.; Perros, A. P.; Myllyperkiö, P.; Kurotobi, K.; Lipsanen, H.; Imahori, H.; Lemmetyinen, H.; Tkachenko, N. V. Photo-Induced Electron Transfer at Nanostructured Semiconductor–Zinc Porphyrin Interface. *Chem. Phys. Lett.* **2014**, *592*, 47–51.

(30) Grätzel, M. Photoelectrochemical cells. *Nature* **2001**, *414*, 338–344.

(31) Imahori, H.; Tamaki, K.; Guldi, D. M.; Luo, C.; Fujitsuka, M.; Ito, O.; Sakata, Y.; Fukuzumi, S. Modulating Charge Separation and Charge Recombination Dynamics in Porphyrin-Fullerene Linked Dyads and Triads: Marcus-Normal versus Inverted Region. *J. Amer. Chem. Soc.* **2001**, *123*, 2607–2617.

(32) Dubey, R. K.; Niemi, M.; Kaunisto, K.; Efimov, A.; Tkachenko, N. V.; Lemmetyinen, H. Direct Evidence of Significantly Different Chemical Behavior and Excited-State Dynamics of 1,7- and 1,6-Regioisomers of Pyrrolidinyl-Substituted Perylene Diimide. *Chem. Eur. J.* **2013**, *19*, 6791–6806.

(33) KC, C. B.; Stranius, K.; D'Souza, P.; Subbaiyan, N. K.; Lemmetyinen, H.; Tkachenko, N. V.; D'Souza, F. Sequential Photoinduced Energy and Electron Transfer Directed Improved Performance of the Supramolecular Solar Cell of a Zinc Porphyrin-Zinc Phthalocyanine Conjugate Modified TiO_2 Surface. *J. Phys. Chem. C* **2013**, *117*, 763–773.

Graphical TOC Entry